# The equilibrium properties of charged hard spheres with adhesive interactions between oppositely charged ions

Jayendran C. Rasaiah and Song Hi Lee
*Thermophysics Division, National Bureau of Standards, Gaithersburg, Maryland 20899* [a)]

(Received 3 July 1985; accepted 5 September 1985)

The equilibrium properties of charged hard spheres with adhesive interactions between oppositely charged ions are studied in the hypernetted chain/mean spherical (HNC/MS) approximation and in the Percus–Yevick/Mean spherical (PY/MS) approximation which are solved analytically. Numerical solutions to the hypernetted chain (HNC) approximation for this model are also compared with the HNC/MS approximation for a model 2–2 electrolyte in the preparative concentration range. The effect of adhesion on the low density phase transition of the primitive model electrolyte is found to be slight in contrast to the effect of charge on the phase separations at high densities of a two component mixture of hard spheres in which there is adhesion only between molecules of different species.

## I. INTRODUCTION

The properties of adhesive hard spheres have been discussed by Baxter[1] in the Percus–Yevick (PY) approximation and Waisman and Lebowitz[2] have studied the restricted primitive model (RPM) for charged hard spheres in the mean spherical (MS) approximation. In this paper we investigate adhesive charged hard spheres when adhesiveness is present only between oppositely charged ions at contact. We have recently investigated electrolytes[3,4] in which oppositely charged ions can form a bond at a distance $L$, where $a/3 < L < a/2$ and $a$ is the diameter of the ions. The present model differs from the previous ones[3,4] studied by us in that there is no steric hindrance to polymerization. Of the approximations that we use in our work, the HNC (hypernetted chain) approximation is solved numerically and the hypernetted chain–mean spherical (HNC/MS) approximation and the Percus–Yevick–mean spherical (PY/MS) approximation are solved analytically. In the HNC/MS approximation, the adhesiveness at contact is treated in the HNC approximation while the remaining interactions are treated in the MS approximations. In the Percus–Yevick–mean spherical (PY/MS) approximation, the PY approximation replaces the HNC approximation for the adhesiveness between oppositely charged ions. The analytic solutions that we obtain for the HNC/MS and PY/MS approximations are found to bear a close resemblance to the solution of the mean spherical approximation for the restricted primitive model electrolyte.

There are several interesting problems that can be explored with this model. When the charges on the ions are turned off we are left with a mixture of two species in which there is adhesion between the different species A and B but not between the A's or the B's alone. We study the phase transition for this system in the PY approximation and observe the changes that occur in the phase diagram when charges of opposite sign are added to the A's and B's, respectively, keeping the solution electrically neutral (the charge–charge interactions are treated in the MS approximation). This transition is found to occur below a definite critical temperature at moderately high densities ($\eta = \pi\rho a^3/6 = 0.3$ where $\rho$ is the total density). In contrast to this there is also evidence for a low density ($\eta = 0.008$) phase transition in the RPM electrolyte.[5] We explore this in the MS approximation before and after adding stickiness (treated in the HNC approximation) to the oppositely charged ions. We find that the addition of charges to the A's and B's shifts the high density critical point and the coexistence curve of the sticky A–B transition, while the introduction of adhesion of comparable strength to oppositely charged ions has only a slight effect on the low density phase transition of the restricted primitive model electrolyte.

The Mayer $f$ function for the interactions between the ions is given by

$$f_{ij}(r) = \xi a(1-\delta_{ij})\delta(r-a)/12 - 1 \quad (0<r<a), \tag{1.1a}$$

$$= \exp[e_i e_j/(\epsilon_0 kTr)] - 1 \quad (r>a), \tag{1.1b}$$

where $r$ is the distance between the ions $i$ and $j$, $e$ is the charge on ion $i$, $a$ is the diameter of the ions, $\epsilon_0$ is the dielectric constant of the solvent, $\delta_{ij}$ is a Kronecker delta, and $\delta(r-a)$ is a delta function. The parameter $\xi$ is the sticking coefficient which measures the strength of the bonding or adhesiveness between unlike ions $(+,-)$; it is the inverse of the parameter $\tau$ used by Baxter[1] in his study of adhesive hard spheres. When $\xi = 0$ the system is identical to the RPM electrolyte. Turning on the adhesiveness alters the Mayer $f$ function for unlike ions and a variation $\delta\xi$ in the sticking coefficient causes a corresponding variation in the $f$ function:

$$\delta f_{ij}(r) = a\delta\xi\,(1-\delta_{ij})\delta(r-a)/12\,. \tag{1.2}$$

To obtain the Helmholtz free energy $A$ of this sticky (or adhesive) electrolyte model (SEM) we consider the functional derivative of the free energy with respect to $f_{ij}(r)$ which is

$$\delta(\beta A/V)/\delta f_{ij}(r,\xi) = -\tfrac{1}{2}\eta\, y_{ij}(r;\xi)\,, \tag{1.3}$$

where the cavity function $y_{ij}(r,\xi)$ is related to the distribution function $g_{ij}(r) = 1 + h_{ij}(r)$ by

$$g_{ij}(r,\xi) = [1 + f_{ij}(r,\xi)]\, y_{ij}(r,\xi)\,, \tag{1.4}$$

---

[a)] Permanent address: Department of Chemistry, University of Maine, Orono, Maine 04469.

in which we have explicitly included the functional dependence on $\xi$. Combining Eq. (1.2) and Eq. (1.3), integrating over $r$, and summing over $i$ and $j$ we find that

$$\beta[A(\mathrm{SEM}) - A(\mathrm{RPM})]/N = -\tfrac{1}{2}\eta \int_0^{\xi} y_{+-}(a,\xi')\,d\xi' . \tag{1.5a}$$

Differentiating with respect to $\rho$ we get the pressure difference

$$[P(\mathrm{SEM}) - P(\mathrm{RPM})]/\rho kT = -\frac{1}{2}\eta \int_0^{\xi} [y_{+-}(a,\xi') + \partial y_{+-}(a,\xi')/\partial\rho]\,d\xi' . \tag{1.5b}$$

The osmotic coefficient $\phi = P/\rho kT$.

The delta function in the Mayer $f$ function for oppositely charged ions implies the presence of a delta function in the correlation functions for oppositely charged ions with a different coefficient $\lambda$ called the association parameter. The correlation function $h_{ij}(r)$ for $r<a$ has the form

$$h_{ij}(r) = -1 + a\lambda(1-\delta_{ij})\delta(r-a)/12 \quad (r<a) . \tag{1.6}$$

The average number $\langle N\rangle$ of ions of opposite sign bonded to an ion is given by $\langle N\rangle = \eta\lambda$ and the reduced association constant

$$K = \frac{\pi\lambda}{3(1-\langle N\rangle)^2} . \tag{1.7}$$

Chemical association between uncharged molecules A and B, where binding occurs at distances $r = a/2$ and $r = a/3$, has been discussed by Cummings and Stell,[6] and the definitions of $\langle N\rangle$ and $K$ used here are the same except that they are specialized to adhesiveness or bonding at contact. The sticking coefficient is related to the association parameter by

$$\lambda = \xi y_{+-}(a,\xi) \tag{1.8}$$

which follows from Eqs. (1.2), (1.4), and (1.6). The function $y_{+-}(a,\xi)$ is determined by the approximation (HNC or PY) used for the adhesiveness at contact. It follows from this that Eq. (1.5a) for the free energy of adhesive charged hard spheres can also be written in the form

$$\beta[A(\mathrm{SEM}) - A(\mathrm{RPM})]/N = -[1 - \ln y_{+-}(a,\lambda)] - \nu\int_0^{\lambda} \ln y_{+-}(a,\lambda')\,d\lambda' , \tag{1.9}$$

where $\nu = \eta\lambda/2$. For an uncharged system this is equivalent to determining the free energy by integration over the inverse temperature. Watts *et al.*[7] have shown that the thermodynamic properties determined through the virial and compressibility equations are very different from those determined from the energy equation when the PY approximation is employed for adhesive hard spheres. However, we determine the free energy differences between charged and uncharged adhesive hard spheres using Eqs. (1.5a) or (1.9). These equations are known to yield good results[4] for sticky electrolytes in the preparative concentration range when the HNC/MS approximation is used and the stickiness occurs at a distance less than the molecular diameter. We have no corresponding information on the PY/MS approximation at liquid densities so the accuracy of our results for the phase transition at these densities should be treated with caution. However, our estimates of the shifts in the critical parameters on adding charge may be more accurate than the absolute values themselves. The chemical potential $\mu$ in the SEM is given by

$$\mu(\mathrm{SEM}) = A(\mathrm{SEM})/N + P(\mathrm{SEM})/\rho . \tag{1.10}$$

The phase diagrams were determined from an analysis of $\mu$ vs $P$ and $P$ vs $\xi$.

In Sec. II of this paper we discuss details of the solution for adhesive charged hard spheres in the HNC/MS and PY/MS approximations. The results for these approximations and for our numerical solutions to the HNC approximations are presented and discussed in Sec. III.

## II. THE SOLUTION FOR ADHESIVE CHARGED HARD SPHERES IN THE HNC/MS AND THE PY/MS APPROXIMATIONS

As discussed elsewhere,[3,4] the Ornstein–Zernike equation for a symmetrical electrolyte can be written as two separate equations for the sums and differences, respectively, of the correlation functions:

$$h_S(r) = c_S(r) + \rho\int c_S(s)h_S(|\mathbf{r}-\mathbf{s}|)\,ds , \tag{2.1a}$$

$$h_D(r) = c_D(r) - \rho\int c_D(s)h_D(|\mathbf{r}-\mathbf{s}|)\,ds , \tag{2.1b}$$

where

$$c_S(r) = [c_{+-}(r) + c_{++}(r)]/2 , \tag{2.2}$$

$$c_D(r) = [c_{+-}(r) - c_{++}(r)]/2 \tag{2.3}$$

are the sum and difference functions of the direct correlation functions $c_{ij}(r)$ and $h_S(r)$ and $h_D(r)$ are defined similarly. For the model considered here we have the exact relations

$$h_S(r) = -1 + a\lambda\delta(r-a)/24 \quad (r<a) , \tag{2.4}$$

$$h_D(r) = a\lambda\delta(r-a)/24 \quad (r<a) \tag{2.5}$$

which follow from Eq. (1.6). In the MS approximation

$$c_S(r) = 0 \quad (r>a) , \tag{2.6}$$

$$c_D(r) = e^2/(\epsilon_0 kTr) \quad (r>a) , \tag{2.7}$$

where $\epsilon_0$ is the dielectric constant of the solvent background, and $e$ is the magnitude of the charge on the ions.[8]

Baxter[9] has shown that Wiener–Hopf factorization of Eq. (2.1a) leads to the pair of equations:

$$rc_S(r) = q_S'(r) + 2\pi\rho\int_r^{\infty} q_S'(t)q_S(r-t)\,dt , \tag{2.8}$$

$$rh_S(r) = q_S'(r) + 2\pi\rho\int_0^{\infty} q_S(t)(r-t)h_S(|r-t|)\,dt , \tag{2.9}$$

where $q_S(r)$ is zero for $r<0$. The MS closure [Eq. (2.6)] inserted in Eq. (2.8) shows that $q_S(r) = 0$ for $r>a$. The integrated form of Eq. (2.9) is

$$J_S(r) = q_S(r) + 2\pi\rho\int_0^{\infty} dt\, q_S(t)\,J_S(|r-t|) , \quad r>0 , \tag{2.10}$$

where $J_S(r)$ is defined by

$$J_S(r) = \int_r^\infty th_S(t)\, dt\,. \tag{2.11}$$

Since $J_S(a-) = J_S(a+) + \lambda a^2/24$, it follows from Eq. (2.10) that

$$q_S(a-) = \lambda a^2/24\,, \tag{2.12}$$

where we have made use of the fact that $q_S(r) = 0$ for $r > a$. When $0 < r < a$, the solution to Eq. (2.9) is

$$q_S'(r) = Ar + C\,, \tag{2.13}$$

where

$$A = 1 - 2\pi\rho \int_0^a q_S(t)\, dt\,, \tag{2.14}$$

$$C = 2\pi\rho \int_0^a tq_S(t)\, dt\,. \tag{2.15}$$

Integrating Eq. (2.13) and applying the boundary condition (2.12),

$$q_S(r) = A(r^2 - a^2)/2 + C(r-a) + \lambda a^2/24\,, \quad 0 < r < a\,. \tag{2.16}$$

Substituting this into Eqs. (2.14) and (2.15) we find

$$A = (1 + 2\eta - \mu)/(1-\eta)^2\,, \tag{2.17}$$

$$C' = C/a = (\mu - 3\eta)/[2(1-\eta)^2]\,, \tag{2.18}$$

where $\mu = \nu(1-\eta)$ and $\nu = \eta\lambda/2$. When $\lambda = 0$ the coefficients $A$ and $C'$ are identical to those for the PY equation.[9] The contact value of $h_S(a+)$ follows from the Eqs. (2.4), (2.9), and (2.16):

$$h_S(a+) = -1 + D + \nu\lambda/24\,, \tag{2.19}$$

where $D = A(1-\nu/2) + C'(1-\nu) = m - n\lambda$ with $m = (1+\eta/2)/(1-\eta)^2$ and $n = \eta/[2(1-\eta)]$. The function $c_S(r)$ for $0 < r < a$, obtained from Eqs. (2.8) and (2.16), is given by

$$c_S(r) = -\lambda_1 - 6\eta\lambda_2 x - \tfrac{1}{2}\eta\lambda_3 x^3 - \nu\lambda/(24x) \quad (0 < r < a)\,, \tag{2.20}$$

where $x = r/a$, $\lambda_1 = (1 + 2\eta - \mu)(1 + 2\eta - \eta\mu)/(1-\eta)^4$, $\lambda_2 = -(2 + \eta - \mu)^2/[4(1-\eta)^4]$, and $\lambda_3 = A^2 = (1 + 2\eta - \mu)^2/(1-\eta)^4$. A delta function equal to $\lambda a\delta(r-a)/24$ should be added to Eq. (2.20) if the range of $r$ is extended to $r = a$. The expression reduces to the PY result[10,11] when $\lambda = 0$.

The solution to the difference equation follows from an extension of Baxter's analysis to electrolytes.[12,13] It is assumed that

$$c_D(r) = c_D^0(r) + e^2 \exp(-zr)/(\epsilon_0 kTr)\,, \tag{2.21}$$

where $c_D^0(r)$ is a short range function and $z$ is a convergence factor. Wiener–Hopf factorization of the difference equation (2.1b), followed by the limit $z \to 0$ leads to the pair of equations

$$rc_D^0(r) = q_D^{0\prime}(r) + 2\pi\rho\left[Mq_D^0(r) - \int_0^\infty dt\, q_D^{0\prime}(t) q_D^0(t-r)\right]\,, \tag{2.22}$$

$$rh_D(r) = q_D^{0\prime}(r) + 2\pi\rho \int_0^\infty dt\, [q_D^0(t) + M](r-t)h_D(|r-t|)\,, \tag{2.23}$$

where $q_D^0(r) = 0$ for $r < 0$, $M$ is related to the inverse Debye length $\kappa$ by

$$M = -\kappa/(2\pi\rho) \tag{2.24}$$

and $\kappa^2 = 4\pi\rho e^2/(\epsilon_0 kT)$. In the MS approximation,

$$c_D^0(r) = 0 \quad (r > a) \tag{2.25}$$

which implies that [see Eq. (2.22)] $q_D^0(r) = 0$ for $r > a$. The upper limit of integration in Eq. (2.22) is therefore $a+$.

The integrated form of Eq. (2.23) can also be written as

$$J_D(r) = -q_D^0(r) - M/2 + 2\pi\rho \int_0^\infty q_D^0(r) J_D \times(|r-t|)\, dt - \kappa \int_0^r J_D(t)\, dt\,, \tag{2.26}$$

where $J_D(r)$ is defined by

$$J_D(r) = \int_r^\infty th_D(t)\, dt\,. \tag{2.27}$$

In arriving at Eq. (2.26) we have made use of the electroneutrality condition which is equivalent to the relation[3]

$$1 = 4\pi\rho \int_0^\infty J_D(t)\, dt\,. \tag{2.28}$$

The presence of a delta function in $h(r)$ distinguishes $J_D(a+)$ from $J_D(a-)$:

$$J = J_D(a-) = J_D(a+) + \lambda a^2/24\,, \tag{2.29}$$

and it follows from Eqs. (2.26) and (2.29) that

$$q_D^0(r) = -\kappa(r-a) J - \lambda a^2/24 \quad (0 < r < a)\,. \tag{2.30}$$

Using this in Eq. (2.26) with $r = a$, we find a quadratic equation for $J$:

$$\pi\rho a^2\kappa J^2 - (\nu + \kappa a + 1) J + (\kappa a + 2\nu)/(4\pi\rho a) = 0\,, \tag{2.31}$$

whose solution is

$$J = (1 + \nu + \kappa a) - [(1+\nu)^2 + 2\kappa a]^{1/2}/(12\eta\kappa a)\,, \tag{2.32}$$

where $\nu = \eta\lambda/2$ and the negative sign in front of the square root ensures that solution to the RPM in the MS approximation is recovered when $\lambda = 0$. The similarity of our results to the MS-RPM solutions is striking even when $\lambda \neq 0$.

The function $c_D(r)$ for $0 < r < a$ follows from the solution to Eq. (2.22) and Eq. (2.21) with $z = 0$. We find that

$$\begin{aligned} c_D(r) &= \kappa^2 J(1 - \pi\rho Jr) + \lambda\nu a/(24r) \quad (0 < r < a) \\ &= e^2/(\epsilon_0 kTa)[2B - B^2 x] + \lambda\nu/(24x) \quad (0 < r < a)\,, \end{aligned} \tag{2.33}$$

where $x = r/a$, $B = 2\pi\rho Ja$. If we extend the range of $r$ to include $r = a$ a delta function equal to $\lambda a\delta(r-a)/24$ must be added to the expression for $c_D(r)$. The contact value $h_D(a+)$ follows from Eqs. (2.23) and (2.30):

$$h_D(a+) = c_D^0(a-) = e^2(B-1)^2/(\epsilon_0 kTA) - \lambda\nu/24\,, \tag{2.34}$$

where we have used the quadratic equation (2.31) in the form

$$\kappa a(B-1)^2 = 2B(\nu+1) - 2\nu \tag{2.35}$$

to simplify the algebra. It is readily verified that $h_D(r) - c_D(r)$ is continuous at $r = a$. The distribution functions $g_{++}(a+)$ and $g_{+-}(a+)$ at contact [see Eqs. (2.19) and (2.34)] are found to be

$$g_{++}(a+) = D - e^2(1-B)^2/(\epsilon_0 kTa) + \nu\lambda/12\,, \quad (2.36)$$

$$g_{+-}(a+) = D + e^2(1-B)^2/(\epsilon_0 kTa)\,. \quad (2.37)$$

This completes our analysis of the charge–charge interactions for this model treated according to the mean spherical approximation. When $\lambda = 0$ the solutions to the MSA for the RPM are recovered. When $\lambda = 1/\eta$ we have the solutions in the MSA for adhesive hard spheres in which, on the average, every ion is bonded to at least one other ion of opposite sign.

We next consider approximations for the adhesiveness at contact between oppositely charged ions when there is a mixture of free and associated ions $(0 < \lambda < 1/\eta)$. Since $\xi = 1/\tau$, Eq. (1.8) is equivalent to

$$\lambda\tau = y_{+-}(a+)\,. \quad (2.38)$$

In the PY/MS approximation,

$$\begin{aligned}\lambda\tau &= g_{+-}(a+) - c_{+-}(a+)\\ &= g_{+-}(a+) - e^2/(\epsilon_0 kTa)\\ &= D + e^2(B^2 - 2B)/(\epsilon_0 kTa)\,, \end{aligned}\quad (2.39)$$

which leads to the following cubic equation for $\nu$:

$$\begin{aligned}(2c-4)\nu^3 + (c^2 + 2b - 6 - 2x)\nu^2 + (2bc - 4 - 4x)\nu\\ + b^2 - 2x - 1 = 0\,,\end{aligned}\quad (2.40)$$

where

$$b = 1 + 6\eta(2+\eta)/(1-\eta)^2 + (2x - x^2)/2\,, \quad (2.41)$$

$$c = (-24\tau - 14\eta + 2)/(1-\eta)\,. \quad (2.42)$$

The smallest real solution corresponds to the one obtained when the charge is zero (when the cubic equation becomes a linear equation) and is taken as the physically relevant one for this approximation. In the HNC/MS approximation

$$\begin{aligned}\lambda\tau &= \exp[h_{+-}(a+) - c_{+-}(a+)]\\ &= \exp[D + e^2(B^2 - 2B)/(\epsilon_0 kTa) - 1]\end{aligned} \quad (2.43)$$

which is solved for $\lambda$ iteratively. Again the smallest real solution is taken as the physically relevant one. The free energy difference between the adhesive or sticky electrolyte model is calculated from Eqs. (1.5) or (1.9); in the HNC/MS approximation the integration is easily done analytically and we find that

$$\beta[A\,(\mathrm{SEM}) - A\,(\mathrm{RPM})]/N = -\eta\, I\,(\mathrm{HNC/MSA})/2\,, \quad (2.44)$$

where

$$\begin{aligned} I\,(\mathrm{HNC/MS}) = \lambda + \frac{\eta\lambda^2}{4(1-\eta)} - \frac{\lambda^2}{24} - \frac{\eta\lambda^3}{72}\\ \times\frac{[(\eta\lambda/2+1)^2 + 2x]^{1/2}}{36\eta^2}(\eta^2\lambda^2 + \eta\lambda - 2 - 4x)\\ + \frac{(1+2x)^{1/2}}{18\eta^2}\,. \end{aligned}\quad (2.45)$$

In the PY/MS approximation the integrations in Eqs. (1.5) or (1.9) have to be done numerically. However, to use these expressions we need the Helmholtz free energy of the RPM electrolyte in the MSA which, from the analysis of Waisman and Lebowitz,[2] is known to be

$$\begin{aligned}\beta[A\,(\mathrm{RPM}) - A^0]/N\\ = [-6x + 3x^2 + 2 - 2(1+2x)^{3/2}]/(72\eta)\,.\end{aligned} \quad (2.46)$$

The pressure in the MS approximation is

$$\begin{aligned}\beta[P\,(\mathrm{RPM}) - P^0]/\rho\\ [3x + 3x(1+2x)^{1/2} + -2(1+2x)^{1/2} + 2]/(72\eta)\,,\end{aligned} \quad (2.47)$$

In Eqs. (2.46) and (2.47) the superscript zero refers to the properties of the hard sphere system in the Percus–Yevick approximation, but we use the Carnahan and Starling[14] equation which is more accurate for the pressure and free energy of hard spheres:

$$\beta P^0/\rho = (1 + \eta + \eta^2 - \eta^3)/(1-\eta)^3\,, \quad (2.48)$$

$$\beta A^0/N = \ln\eta + \eta(4 - 3\eta)/(1-\eta)^2\,. \quad (2.49)$$

The excess energy of adhesive electrolytes is given by[3]

$$\beta E^{\mathrm{ex}}/N = \langle N\rangle(d\ln\tau/d\ln\beta)/2 - \kappa a H'/2\,, \quad (2.50)$$

where

$$\begin{aligned} H' &= J_D(a+)/a\\ &= \{(1+\nu) + \kappa a(1-\nu) - [(1+\nu)^2 + 2\kappa a]^{1/2}\}/(12\eta)\,.\end{aligned} \quad (2.51)$$

In the saturation limit $\langle N\rangle = \lambda\eta = 1$, $\nu = 1/2$, and

$$H' = [3/2 + \kappa a/2 - (9/4 + 2\kappa a)^{1/2}]/(12\eta)\,. \quad (2.52)$$

At zero charge the adhesive electrolyte becomes an adhesive (or sticky) nonelectrolyte (SN) and the mean spherical approximation for the RPM electrolyte becomes identical to the Percus–Yevick approximation for hard spheres. It follows from Eqs. (2.43) and (2.39) that the free energy difference between the sticky nonelectrolyte (SN) and hard spheres (HS) can also be obtained analytically in the HNC/PY approximation and in the PY approximation. We find that: (a) in the HNC/PY approximation,

$$\beta[A\,(\mathrm{SN}) - A^0]/N = -\frac{\eta}{2}\left[\lambda + \frac{\lambda^2}{4(1-\eta)}\right], \quad (2.53)$$

where $\lambda\tau = \exp[D-1]$. Differentiating with respect to the density and taking note that, for the SN system,

$$\frac{d\lambda}{d\eta} = \frac{[5 + \eta - \lambda(1-\eta)]}{2(1-\eta)^3 + \lambda\eta(1-\eta)^2}\,, \quad (2.54)$$

the pressure in the HNC/PY approximation is given by

$$\begin{aligned}\frac{\beta(P-P^0)}{\rho} = \tfrac{1}{2}\eta\left\{\lambda + \frac{\lambda^2(2-\eta)}{4(1-\eta)}\right.\\ \left. + \frac{\eta\lambda[2 + \eta(\lambda-2)][5 + \eta - \lambda(1-\eta)]}{4(1-\eta)^4 + 2(1-\eta)^3}\right\}.\end{aligned} \quad (2.55)$$

(b) In the PY approximation, $\lambda\tau = D$ and we find

$$\beta[A\,(\mathrm{SN}) - A^0]/N = -\frac{\eta m}{2n}\ln\frac{(1+n\lambda)}{m}\,, \quad (2.56)$$

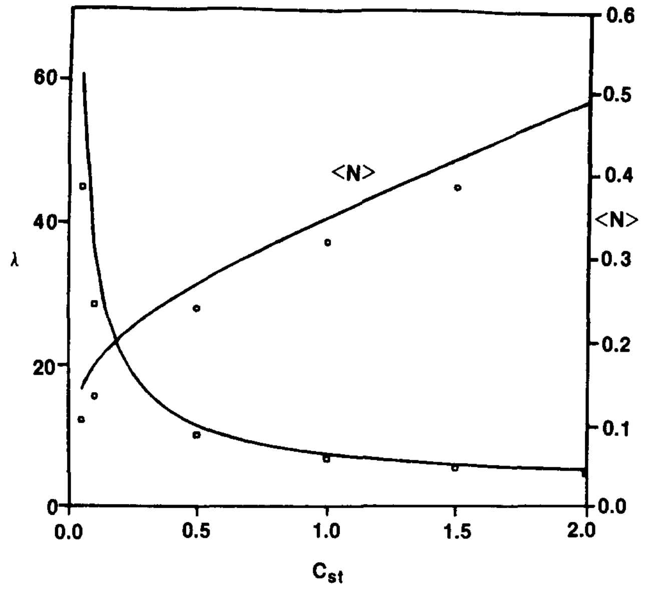

FIG. 1. Plots of $\lambda$ and $\langle N \rangle$ as a function of concentration for the adhesive charged hard sphere 2–2 electrolyte. The temperature $T = 298$ K, $\epsilon_0 = 78.358$, $a = 4.2$ Å, and the inverse of the sticking coefficient $\tau = 0.91 \times 10^{-3}$.O and □: HNC approximation;—HNC/MS approximation.

$$\frac{d\lambda}{d\eta} = \frac{\lambda(\eta+2)[\eta+5-\lambda(1-\eta)]}{(1-\eta)[2+\eta-2\lambda\eta(1-\eta)]^2}, \tag{2.57}$$

and

$$\frac{\beta(P-P^0)}{\rho} = -s\left[\ln\left(1+\frac{n\lambda}{m}\right) + \frac{m}{n(1+n\lambda/m)}\right] + \frac{1}{(1+n\lambda/m)}\frac{d\lambda}{d\eta}, \tag{2.58}$$

where $s = (\eta^2 + 4\eta - 2)/[\eta^2(\eta - 1)^2]$, and $n$ and $m$ are defined below Eq. (2.19).

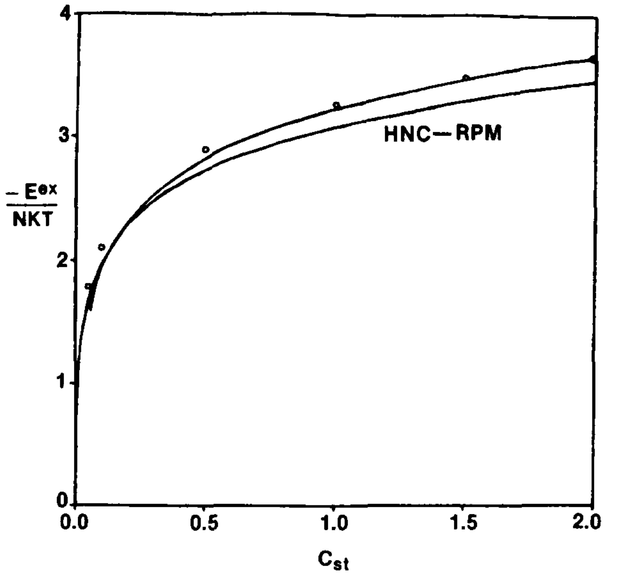

FIG. 2. $E^{ex}/NkT$ as a function of the concentration in the HNC and HNC/MS approximations for the RPM and the adhesive charged hard sphere model. O: HNC approximation;—HNC/MS approximation. (See caption of Fig. 1 for details of the molecular parameters.)

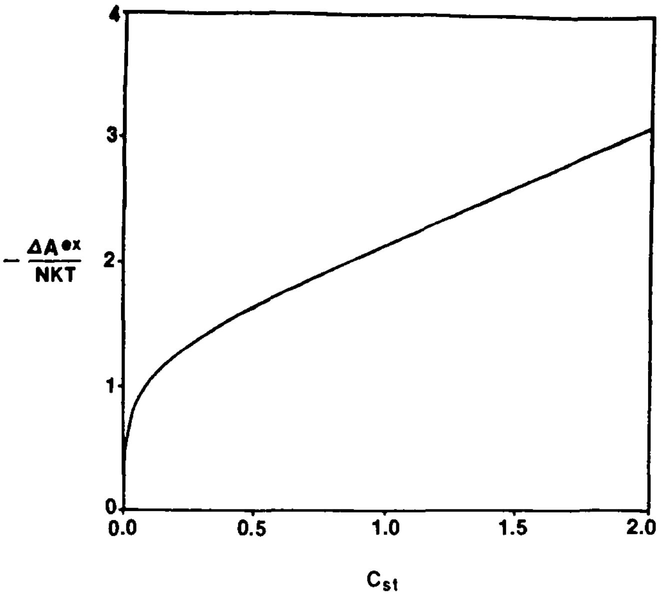

FIG. 3. $\Delta A^{ex}/NkT$ as a function of the concentration for the RPM and the adhesive charged hard sphere model in the HNC/MS approximation. $\Delta$ = SEM–RPM. (See caption of Fig. 1 for details of the molecular parameters.)

## III. RESULTS AND DISCUSSION

Our calculations explore three systems that are related but exhibit different equilibrium properties:

(a) A model 2–2 electrolyte with adhesiveness between oppositely charged ions (HNC and HNC/MS approximations).

(b) The high density phase transition for hard spheres and charged hard spheres in which there is adhesion between species A and B but not between the individual A's or the B's (PY/MS approximation).

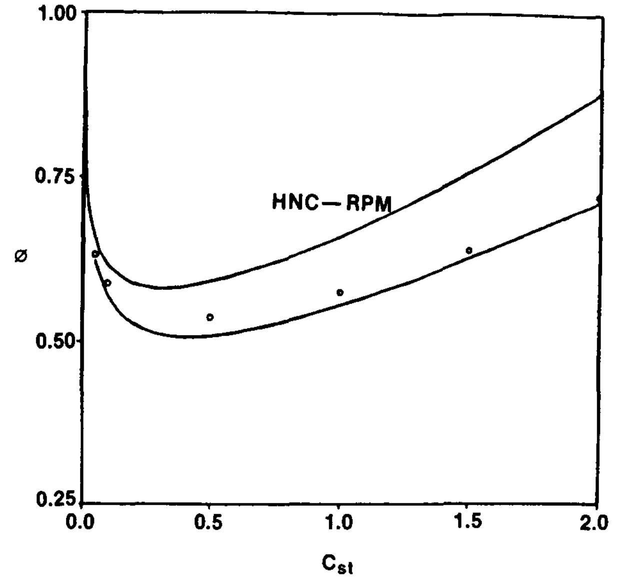

FIG. 4. The osmotic coefficient $\phi$ as a function of the concentration for the RPM and SEM (adhesive charged hard spheres in the HNC and HNC/MS approximations. O: HNC approximation (virial equation).—:HNC/MS approximation [Eq. (1.5b)]. (See caption of Fig. 1 for details of the molecular parameters.)

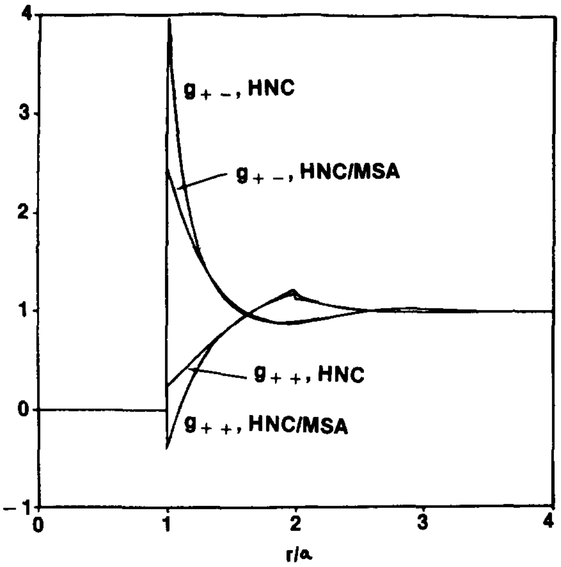

FIG. 5. Distribution functions for a 2–2 model adhesive charged hard sphere electrolyte at 2.0 molar in the HNC and HNC/MS approximations. (See caption of Fig. 1 for details of the molecular parameters.)

(c) The effect of adhesiveness between oppositely charged ions on the low density phase transition of the RPM electrolyte (HNC/MS approximation).

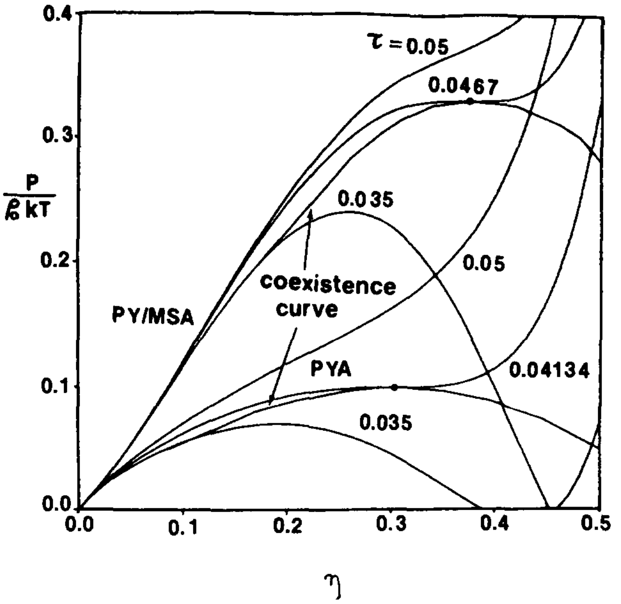

FIG. 6. The phase diagram in the $P/\rho_0 kT-\eta$ plane for adhesive hard spheres (PY approximation) and adhesive charged hard spheres (PY/MS approximation) where $\rho_0 = 6/(\pi a^3)$. The ionic parameters ($e = 1$ esu, $a = 4.2$ Å, $\epsilon_0 = 78.358$) correspond to a reduced temperature $T^* = (\epsilon_0 kTa/e^2) = 0.5865$. The values of $\tau$ are 0.05, 0.041 34, 0.035 for the uncharged system and 0.05, 0.0467, 0.035 for the charged system. The critical constants are in Table I.

TABLE I. Critical constants for high density phase transition $\eta = 0.304$.

| | PY[a] | PY/MS[b] |
|---|---|---|
| $\eta_c$ | 0.304(0.32) | 0.375 |
| $\tau_c$ | 0.041 34(0.1185) | 0.0467 |
| $P_c/\rho_c kT$ | 0.329(0.32) | 0.880 |
| $\lambda_c$ | 9.156(5.761) | 4.537 |

[a] Hard sphere mixtures with adhesion between unlike particles A and B. The numbers in parentheses are the critical constants and parameters for the corresponding one component system studied by Baxter (Refs. 1 and 13).

[b] Charged hard spheres with adhesion between + and − ions ($T^* = 0.5865$).

The details of the numerical methods used to solve the hypernetted chain (HNC) approximation for the charged hard spheres with stickiness between oppositely charged ions are discussed elsewhere[4] and are easily extended to the present model. The parameters for the model 2–2 electrolyte are chosen as before[3,4]; $a = 4.2$ Å, $T = 298$ K, $\epsilon_0 = 78.358$, and $\tau = 1/\xi$ is determined from the relation[3]

$$\tau = \frac{L^3}{12L^2 w + w^3} \exp(-\epsilon_2/kT), \tag{3.1}$$

where $L = a$ is the distance at which oppositely charged ions stick, $w = 0.1a$, and $\epsilon_2$ is chosen to be 6.82 $kT$ which is the Coulomb energy at contact in a medium of dielectric constant $\epsilon_0 = 78.358$. The calculated $\tau = 0.91 \times 10^{-3}$. We consider Eq. (3.1) and the model from which it is derived[3] as a reasonable way to estimate the parameter $\tau$ for a typical electrolyte solution. The results are summarized in Figs. 1–5. Figure 1 shows that there is a small but significant difference between the association parameter $\lambda$ calculated according to the HNC and HNC/MS approximations when $L = a$. This is in contrast to calculations of the association parameter at $L = a/2$ and $a/3$[3,4] when the two approximations gave essentially the same values for $\lambda$. The function $\langle N \rangle$ defined before Eq. (1.7) is also much smaller for the range of concentrations up to 2.0 M studied here with $L = a$ reflecting the smaller values of $\lambda$. In Figs. 2–4 we plot the excess thermodynamic functions against the concentration and Fig. 5 shows the distribution functions for the 2.0 M electrolyte. The HNC and HNC/MS approximations differ most at distances near contact, with $g_{++}(r)$ negative and $g_{+-}(r)$ too small in the HNC/MS approximation in comparison to the HNC approximation. The peak at $r = 3a$ in $g_{++}(r)$ due to linear trimers of alternating opposite charge is reproduced by both approximations which are in close agreement at this distance.

Baxter's study of adhesive hard spheres in the PY approximation[1] treats adhesiveness at contact between the spheres of a one component system. The two component A–B system with adhesiveness only between A and B at contact, which we investigate, also shows a phase transition with a phase diagram that is shifted by the addition of charges of opposite sign to the A's and B's. The critical constants ob-

TABLE II. Critical constants for the low density phase transition $\eta = 0.0076$.

| | MS(RPM) | HNC/MS[a] |
|---|---|---|
| $\eta_c$ | 0.007 6 | 0.007 6 |
| $T_c^*$ | 0.078 58 | 0.078 66 |
| $P_c/\rho_c kT$ | 0.084 7 | 0.085 4 |
| $\lambda_c$ | 0 | 0.020 23 |

[a] Adhesive charged hard spheres ($\tau = 0.041\ 34$).

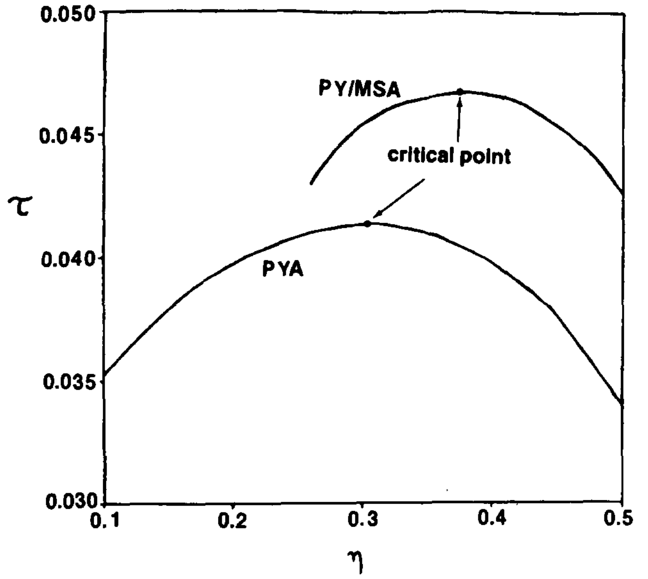

FIG. 7. The phase diagram in the $\tau - \eta$ plane for the adhesive hard sphere system (PY approximation) and the adhesive charged hard sphere system (PY/MS approximation). The ionic parameters (see caption to Fig. 6) correspond to a reduced temperature $T^* = 0.5865$. The critical constants are in Table I.

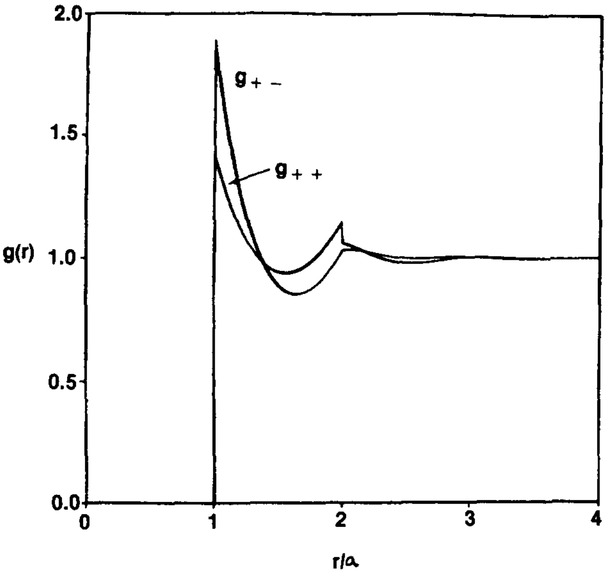

FIG. 9. Distribution functions for adhesive charged hard spheres (PY/MS approximation) at a reduced density of 0.304. The values of $\tau$ and $\lambda$ (in parentheses) are 0.05(3.687), 0.041 34(3.797), 0.035(3.882), with $T^* = 0.5865$.

tained in the PY approximation (uncharged adhesive hard spheres) and the PY/MS approximation (charged adhesive hard spheres) for our A–B system are given in Table I together with the critical constants for the one component adhesive hard sphere system studied by Baxter.[1,9] In Figs. 6 and 7 we have the phase diagrams in the $P - \eta$ and $\tau - \eta$ planes, and in Figs. 8 and 9 the distribution functions for these systems in the vicinity of the critical point. The ion size ($a = 4.2$ Å) and the charge ($e = 1$ esu) of the adhesive charged hard sphere system correspond to a reduced temperature $T^* = (\epsilon_0 kTa/e^2) = 0.5865$. Comparison of Figs. 8 and 9 shows that the addition of charge produces significant changes in the pair correlation functions of adhesive hard spheres. At this density, temperature and ionic charge the association parameter in the PY approximation for the stickiness is positive. However, the low density phase transition of the RPM electrolyte behaves differently when stickiness is added. The PY approximation for stickiness at this reduced temperature and low density leads to negative values for $\lambda$ which are unrealistic.[3] We therefore use the HNC/MS approximation, with an inverse sticking coefficient $\tau$ equal to the critical $\tau_c$ for the

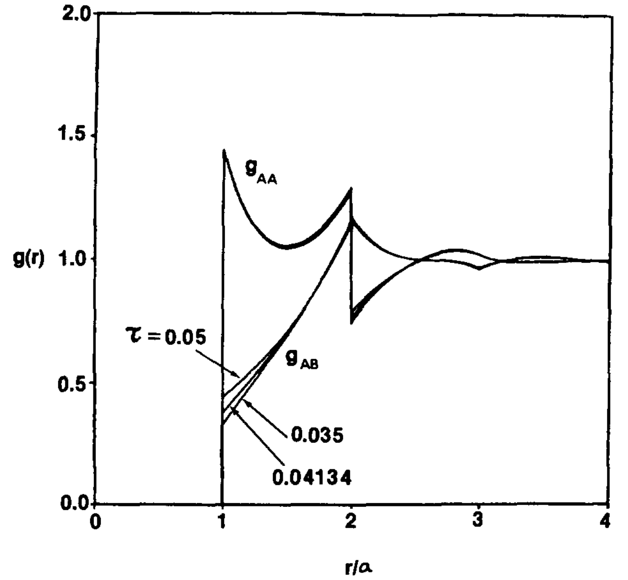

FIG. 8. Distribution functions for adhesive hard spheres (PY approximation) at a reduced density $\eta = 0.304$. The values of $\tau$ and $\lambda$ (in parentheses) are 0.05(8.861), 0.041 34(9.156), 0.035(9.385).

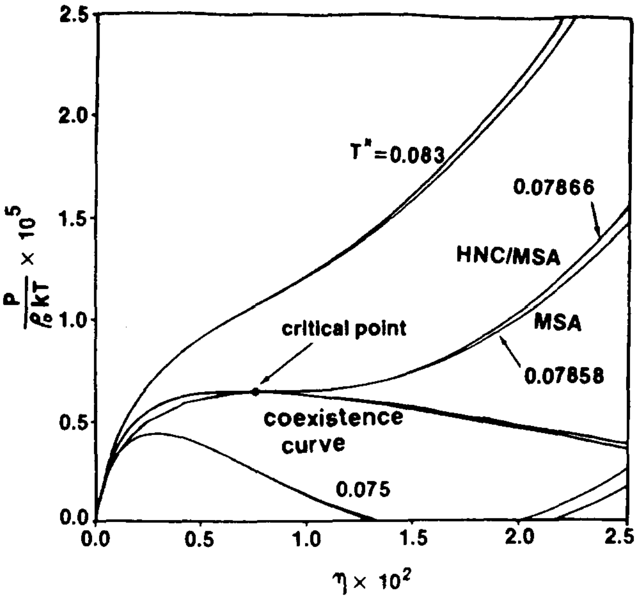

FIG. 10. The low density phase transition in the $P/\rho_0 kT - \eta$ plane for the RPM electrolyte before (MSA) and after (HNC/MS) introducing adhesiveness ($\tau = 0.041\ 34$) between oppositely charged ions where $\rho_0 = 6/\pi a^3$. The values of $T^*$ are 0.083, 0.078 58, 0.075 for the RPM (MSA) and 0.083, 0.078 66, 0.075 for the adhesive charged hard sphere system.

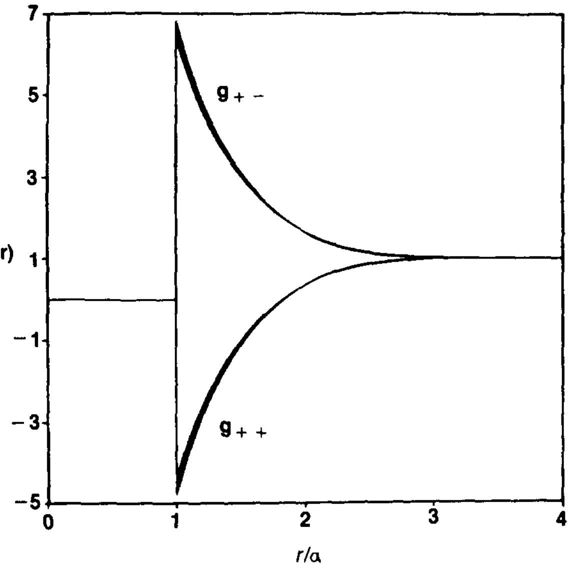

FIG. 11. The ion distribution functions for the adhesive charged hard sphere system depicted in Fig. 10 at a reduced density of $\eta = \pi\rho a^3/6 = 0.0076$. The values of $T^*$ and $\lambda$ (in parentheses) are 0.083 (0.315), 0.078 66 (0.0202), 0.075 (0.0133) with $\tau = 0.0413$.

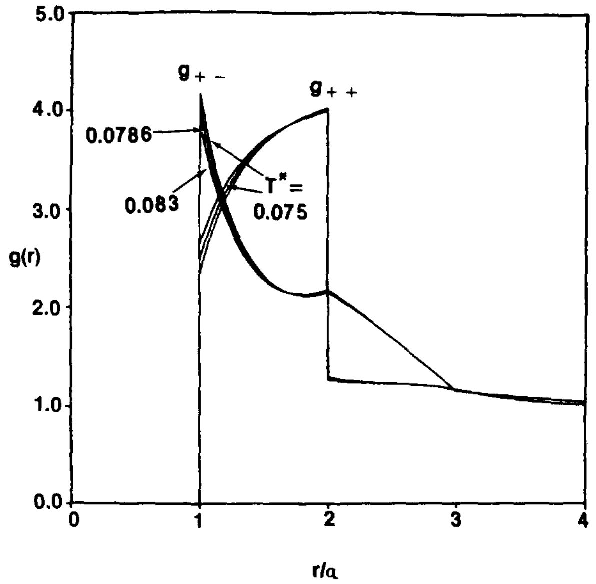

FIG. 13. The ion distribution functions for the adhesive charged hard sphere system depicted in Fig. 12 except that $\lambda = 1/\eta = 131.6$, i.e., $\langle N \rangle = 1$.

high density phase transition, to ensure that the sticking coefficient $\xi$ introduced is nearly the same. The association parameters $\lambda$ which are also functions of the density and the ion interactions turn out to be quite small in comparison to what is found near the high density phase transition. The phase diagrams are shown in Fig. 10 and the critical constants given in Table II. In Figs. 11 and 12 we have the distribution functions before and after adding the adhesiveness to the RPM electrolyte. It is apparent that the phase diagrams and correlation functions near the two phase region are barely altered by the addition of the prescribed adhesiveness. The absence of peaks corresponding to significant amounts of trimers, tetramers, etc. and the smooth and featureless correlation functions for $r > a+$ in the vicinity of the critical point suggest a distribution of dimers and clusters of varying sizes near this low density phase transition. In the limit $\lambda = 1/\eta$ the distribution functions at the critical density shown in Fig. 13 are quite different reinforcing our views about the low density phase transition. The HNC/MS equation cannot be used to check the high density phase transition observed in the PY/MS approximation since the replacement of the PY approximation for adhesion by the HNC approximation does not lead to a well defined critical point at realistic fluid densities and reasonable values of the sticking coefficient.

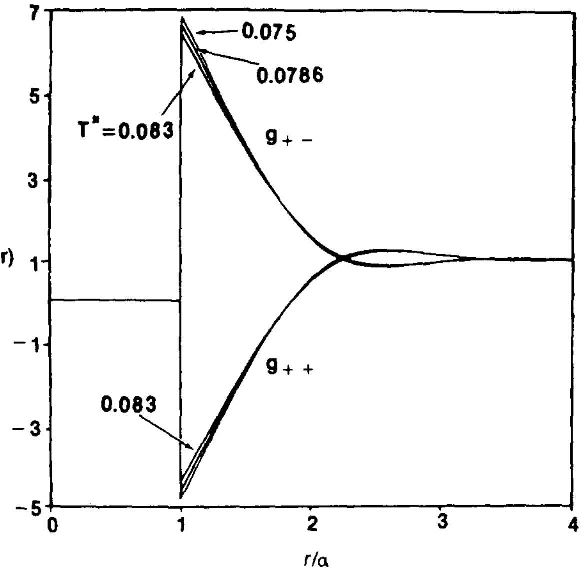

FIG. 12. The ion distribution functions for the charged hard sphere system (RPM) at a reduced density $\eta = 0.0076$. The values of $T^*$ are 0.083, 0.0786, 0.075 and $\lambda = 0$.

## ACKNOWLEDGMENTS

The hospitality and computing facilities at the National Bureau of Standards where this work was done is most gratefully acknowledged. JCR would also like to thank Noel Thompson for helpful discussions of Baxter's work and the Wiener–Hopf factorization for electrolytes during a cold winter in Maine in 1978. This research was supported by a grant from the National Science Foundation CHE-8305747.

[1] R. J. Baxter, J. Chem. Phys. **49**, 2770 (1968).

[2] E. Waisman and J. Lebowitz, J. Chem. Phys. **52**, 4307 (1970); **56**, 3086, 3092 (1972).

[3] S. H. Lee, J. C. Rasaiah, and P. Cummings, J. Chem. Phys. **83**, 317 (1985).

[4] J. C. Rasaiah and S. H. Lee, J. Chem. Phys. **83**, 5870 (1985).

[5] G. Stell, K. C. Wu, and B. Larsen, Phys. Rev. Lett. **37**, 1369 (1976).

[6] P.T. Cummings and G. Stell, Mol. Phys. **51**, 253 (1984). There are several other statistical mechanical studies of chemical association; the earliest, to our knowledge, is the work of L. Boltzmann (1898) reported in *Lectures on Gas Theory Part II*, translated by S. G. Bush (University of California, Berkeley, 1964), Chap. 6. Other important work in this field may be found in the following papers: (a) H. C. Andersen, J. Chem. Phys. **59**, 4717 (1973); (b) D. Chandler and L. R. Pratt, *ibid.* **65**, 2925 (1976); (c) J. S. Høye

and K. Olaussen, Physica A **104**, 435 (1980). For an excellent review see the article by D. Chandler, in *Studies in Statistical Mechanics—Vol. VIII; The Liquid State of Matter: Fluids, Simple and Complex*, edited by E. W. Montroll and J. L. Lebowitz (North-Holland, Amsterdam, 1982).

[7] R. O. Watts, D. Henderson, and R. J. Baxter, Adv. Chem. Phys. **21**, 432 (1971).

[8] The asymptotic form of the direct correlation function is modified in the limit of complete dimerization (Ref. 4). Its effect is likely to be small in the systems studied by us and we ignore any deviation from Eq. (2.7). Alternatively we take Eq. (2.7) as our definition of the MSA for these systems.

[9] R. J. Baxter, Aust. J. Phys. **21**, 563 (1968).

[10] M. Wertheim, (a) Phys. Rev. Lett. **10**, 321 (1963); (b) J. Math. Phys. **5**, 643 (1964).

[11] E. Thiele, J. Chem. Phys. **39**, 474 (1963).

[12] L. Blum (a) Mol. Phys. **30**, 1529 (1975), (b) *Theoretical Chemistry: Advances and Perspectives*, edited by H. Eyring and D. Henderson (Academic, New York, 1980), Vol. 5, pp. 1–66.

[13] N. Thompson, University of Maine, Chemistry Department Report No. 2001 (1978).

[14] N. F. Carnahan and K. E. Starling, J. Chem. Phys. **51**, 635 (1969).